Journal of Power Sources 183 (2008) 174–181

Contents lists available at ScienceDirect

Journal of Power Sources

journal homepage: www.elsevier.com/locate/jpowsour

# Surface modifications of aluminum alloy 5052 for bipolar plates using an electroless deposition process

Ching-Yuan Bai[a], Yu-Hsien Chou[b], Chu-Lung Chao[a], Shuo-Jen Lee[c], Ming-Der Ger[a,*]

[a] Department of Applied Chemistry & Materials Science, Chung Cheng Institute of Technology, National Defense University, Ta-His, Tao-Yuan, 335, Taiwan, ROC
[b] Graduate School of Defense Science, Chung Cheng Institute of Technology, National Defense University, Ta-His, Tao-Yuan, Taiwan, ROC
[c] Department of Mechanical Engineering, Yuan Ze Fuel Cell Center, Yuan Ze University, Tao-Yuan, Taiwan, ROC

ARTICLE INFO

*Article history:*
Received 3 March 2008
Received in revised form 25 April 2008
Accepted 25 April 2008
Available online 7 May 2008

*Keywords:*
Electroless deposition
Ni–Mo–P alloys
Corrosion resistance
Thermal stability

ABSTRACT

This study tries to replace graphite bipolar plates in fuel cells with surface-modified aluminum alloy 5052. To improve the surface characteristics of Al alloy, Ni–Mo–P coatings were deposited on the substrates under various pH values and concentrations of sodium molybdate ($Na_2MoO_4$) by an electroless deposition process. The effects of the controlling conditions on the microstructure and the corrosion resistance of these deposits were examined. Moreover, the thermal stability and the corrosion resistance of Ni–Mo–P coatings were compared with those of Ni–P deposits in various attacking environments. The experimental results indicate that the electrical conductivity of all deposits produced in this experiment is superior to the U.S. DOE's target. The optimum Ni–Mo–P coating, which is produced in a solution containing $4.13 \times 10^{-2}$ M $Na_2MoO_4$ at pH 7.0 and 70 °C, possesses superior corrosion resistance in a mixed acidic environment. It is also found that Ni–Mo–P coatings exhibit better thermal stability, and superior long-term corrosion resistance than Ni–P deposits. The Ni–Mo–P deposits, therefore, are promising for applications in protecting coatings for bipolar plates.



## 1. Introduction

The crisis of global warming and the impending exhaustion of fossil fuels have already become the most important and urgent issue for mankind. Development of energy systems with high efficiency and low pollution, therefore, is a very imperative subject in recent years. Fuel cells, a new kind of energy technology, are expected to play a major role in the economy of energy in this century and for the foreseeable future. Proton-exchange membrane fuel cells (PEMFCs) are one of the most valuable fuel cell systems. PEMFCs with the advantage of working at a low temperature can start quickly and convert hydrogen and oxygen (or air) to electricity with water as the only residual product [1]. Consequently, PEMFCs have received a great deal of attention from the research community of fuel cells mainly because of their very low pollution in the consideration of environmental protection.

In the PEM fuel cell systems, bipolar plates are one of the significant parts of the cell stack [2–5]. Conventionally, bipolar plates were fabricated with graphite because of its chemical nobility as well as high electrical and thermal conductivity. However, graphite bipolar plates make up about 80% of the fuel cell stack's mass and volume. This results in large weights, great sizes, and high fabricating costs of fuel cells, and thus impedes the commercial feasibility of fuel cells [6]. The employment of metallic bipolar plates has received attention recently due to the ease of machining a flow–field pattern into the metal [7–13]. Moreover, superior mechanical properties of metals allow designs of a smaller and thinner stack to reduce the weight and volume of fuel cells.

With the characteristics of lightweight, low density, and high specific strength and rigidity, Al alloy is one of the most attractive metals among all structure materials [10,11]. In view of the practicability and the fabricating cost of fuel cells, inexpensive Al alloys could easily be introduced into the bipolar plate process. However, the inferior corrosion resistance of Al alloy bipolar plates and the high contact electrical resistance induced by the formation of oxide on the Al-alloy surface, unfortunately, degrade the performance of fuel cells. Therefore, plating materials with chemical nobility and high electrical conductivity, such as gold and platinum, should be coated on metallic bipolar plates. However, the cost of depositing such noble metals on bipolar plates even in submicron scales prevents these materials from being used. The electroless depositing process is a coating method that plates the films on substrates by an autocatalytic reaction of coated materials without the use of external electrical powers. This process can provide a uniform deposit

* Corresponding author. Tel.: +886 3 3891716; fax: +886 3 3892494.
*E-mail address:* mdger@ccit.edu.tw (M.-D. Ger).

0378-7753/$ – see front matter © 2008 Elsevier B.V. All rights reserved.
doi:10.1016/j.jpowsour.2008.04.082

regardless of substrate geometry. In addition, the procedure is simple, fast, and very low cost [14–17]. The deposits produced by this method generally show a dense and fine structure with low porosity and have good bonding to the substrate. Therefore, electroless deposits are properly used as protective coatings against corrosion attacks. Recently, some of the commercial electroless Ni-based deposits, such as Ni–P and Ni-B alloys, are extensively employed as coatings for applications in electronic or chemical production due to their superior corrosion resistance and electric conductivity. Moreover, Ni–P deposits alloyed with refractory metals, such as molybdenum, can improve the thermal stability of the alloys [18,19]. Therefore, Ni–Mo–P coatings have a good potential for the applications in bipolar plates.

This work attempts to deposit Ni-based coatings on Al alloys used as bipolar plates in order to improve its surface performances, such as corrosion resistance and electrical conductivity. The Ni–P and Ni–Mo–P coatings were deposited on Al alloy 5052 under various pH values or concentrations of sodium molybdate ($Na_2MoO_4$) in the electroless solution. The effects of the controlling conditions on the corrosion resistance, electrical conductivity, and thermal stability of these deposits are examined. Furthermore, the corrosion resistance of the Ni-based alloys, after long-term immersion in a corrosive solution or testing in different attacking environments, is also investigated.

## 2. Experiments

In the present investigation, Al alloy 5052 was used as the substrate material of bipolar plates. The surface coatings, Ni–Mo–P alloys, were deposited on the substrate under different pH values (pHs 7, 8, and 9) and various concentrations of $Na_2MoO_4$ ($2.07 \times 10^{-2}$ M, $4.13 \times 10^{-2}$ M, and $6.20 \times 10^{-2}$ M) by an electroless deposition process to improve the surface characteristics of Al alloy. For comparison, we also prepared Ni–P deposits in an acidic solution (pH 5) system. The electroless deposition procedures for these deposits are shown in Fig. 1, and the experimental details are described below.

The specimens of aluminum alloy 5052 were pre-treated in three steps prior to the electroless deposition process. Step one: the specimens were immersed in a NaOH base solution (pH 12) for 3 min, and cleaned with deionized water. Step two: a nitric acid solution (30% $HNO_3$) was used to pickle the surface of the specimens for 3 min, and the specimens were cleaned with deionized water again. Step three: surface replacement of Zn was then practiced by dipping the specimens in the Zn electrolyte at pH 10 and 25 °C for 1 min. The Zn electrolyte mainly composed of 0.08 M zinc sulfate, 0.65 M ethylenediaminetetraacetic acid, 0.4 M citric acid, and aqua ammonia. After the Zn replacement procedure, the specimens were immersed into the Ni–P or Ni–Mo–P electroless solution to produce the deposits on the substrates. The operating conditions and composition of the depositing bath for preparing Ni–P and Ni–Mo–P coatings are listed in Table 1.

Potentiodynamic polarization was employed to investigate the general corrosion behaviors of the Ni–P and Ni–Mo–P alloys in a 0.5 M $H_2SO_4$ solution. Additionally, 3.5% saltwater and a 0.5 M $H_2SO_4$ + 10 ppm HF aqueous solution were also used as corrosion electrolytes to evaluate the corrosion resistance of the coatings in various aqueous environments. To compare the long-term corrosion resistance of these deposits, some Ni–P and Ni–Mo–P deposits were immersed in the 0.5 M $H_2SO_4$ solution for 20 h or 40 h before polarization tests in the same solution. An annealing treatment of the Ni–P and Ni–Mo–P alloys were performed at 400 °C to investigate the thermal stability of these deposits. To examine the composition of these deposits, some of the Ni–Mo–P deposits were solved into a 10% nitric acid solution, and then analyzed by an inductively coupled plasma atomic emission spectroscope (ICP-AES).

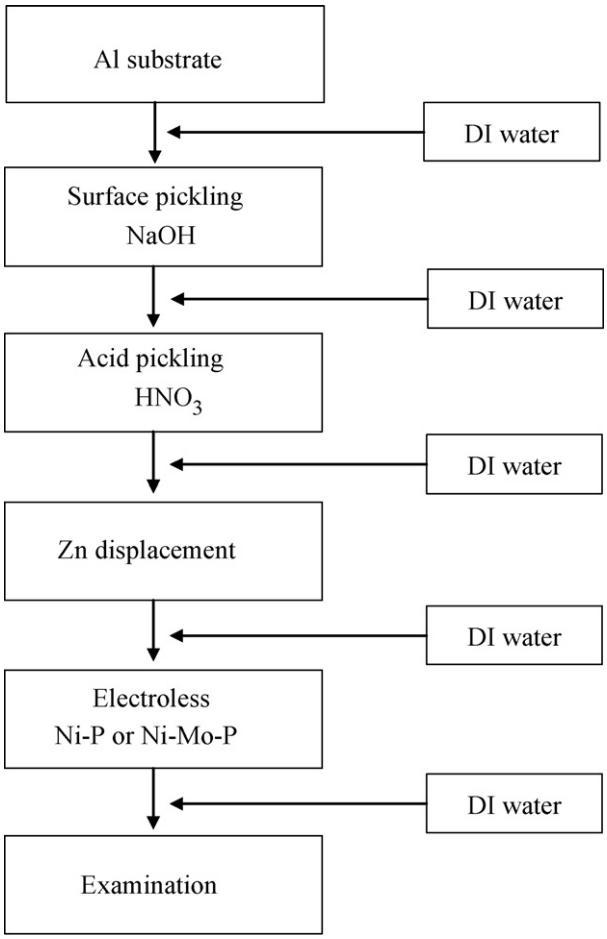


**Fig. 1.** The electroless deposition procedures of Ni–P and Ni–Mo–P deposits.

A four-point probe system was employed to measure the electrical resistivity of the deposited films at a pressure of 100 g tip$^{-1}$, and Vickers hardness tests were performed to measure the microhardness of the deposits. The crystalline structures of all electroless Ni-based alloys prepared in this experiment were analyzed by X-ray diffraction (XRD; using monochromatic Cu Kα radiation with a characteristic wavelength of 1.542 Å). The surface morphology and the microstructure of these deposits were examined by field emission scanning electron microscopy (FE-SEM) with X-ray energy dispersive spectrometry (EDS).

**Table 1**
The plating bath and conditions for preparing Ni–P and Ni–Mo–P deposits

| Chemical compounds | Concentration (M) | |
|---|---|---|
| | Ni–P | Ni–Mo–P |
| $NiSO_4 \cdot 6H_2O$ | 0.114 | 0.114 |
| $Na_2H_2PO_2 \cdot H_2O$ | 0.283 | 0.283 |
| $Na_2MoO_4 \cdot 2H_2O$ | – | $2.07 \times 10^{-2}$ to $6.20 \times 10^{-2}$ |
| Main complex salt (ml l$^{-1}$) | 40 | 40 |
| Auxiliary complex salt | 0.133 | 0.133 |
| Additive (ppm) | 10 | 10 |
| $KIO_3$ (ppm) | 10 | 10 |
| pH | 5 | 7, 8 and 9 |
| Temperature (°C) | 83 | 70 |

## 3. Results and discussion

A qualified coating for bipolar plates has to possess good bonding to the substrate, excellent corrosion resistance, and high electrical conductivity [20,21]. Moreover, the coatings must own superior thermal stability and long-term capability of corrosion resistance in different attacking environments to extend the service life of bipolar plates. To develop such advanced Ni-based coatings (Ni–Mo–P alloys) with these desired properties, we chose pH value and the concentration of sodium molybdate ($Na_2MoO_4$) in the solution as controlling conditions for deposition. The influence of these two deposition parameters on the structure, corrosion resistance in a 0.5 M $H_2SO_4$ solution, and electrical resistance of Ni–Mo–P alloys are examined and discussed. To compare the performance of Ni–Mo–P alloys with that of another extensively used coating, Ni–P alloys, we also prepared Ni–P deposits in an acidic solution (pH 5) system in this study. The thermal stability, the electrical resistance, and the corrosion behavior of Ni–Mo–P alloys in different corrosion environments were investigated and compared with those of Ni–P deposits.

### 3.1. Ni–Mo–P deposits produced in various concentrations of $Na_2MoO_4$

Fig. 2(a)–(c) shows the SEM topographies of the Ni–Mo–P alloys deposited in basic electrolytes (pH 9) with $2.07 \times 10^{-2}$ M, $4.13 \times 10^{-2}$ M, and $6.20 \times 10^{-2}$ M sodium molybdate, respectively, at 70 °C for the same depositing time (60 min). The corresponding cross-sectional SEM images are presented in Fig. 3(a)–(c). The thicknesses of these deposits are approximately 9.5 μm, 4.4 μm, and 4.3 μm, respectively. According to the SEM observation of the Ni–Mo–P deposits, the surface roughness, the granular size, and the thickness of these deposits decreased drastically with increasing concentration of $Na_2MoO_4$, which supplies the Mo element to the Ni–Mo–P alloys, in the electroless bath. This phenomenon may be attributable to the presence of $MoO_4^{2-}$ in the electroless solution [18,19]. In this experiment, the anodic reaction is the oxidation of $H_2PO_2^{2-}$, which is a reducing agent and can be catalyzed to release electrons in the electroless solution for producing the Ni–Mo–P deposits. The $MoO_4^{2-}$ appearing in the solution would cause an inhibiting effect on the oxidation of $H_2PO_2^{2-}$, because $MoO_4^{2-}$ would adsorb on the surface of the substrate [18,19]. In consequence, the catalytic reaction of Ni would be retarded and the deposition rates of Ni–Mo–P alloys would be significantly reduced. The slower deposition rate of Ni–Mo–P results in a smaller granular size and a thinner thickness of these deposits. Consequently, a uniform and dense Ni–Mo–P deposit could be produced by adding suitable amounts of $Na_2MoO_4$ in the deposition solution, although the deposition rates of Ni–Mo–P alloys would be decreased by the inhibiting effect of $MoO_4^{2-}$.

The polarization curves of three Ni–Mo–P deposits, which are produced under various concentration of $Na_2MoO_4$, in a 0.5 M $H_2SO_4$ solution, are shown in Fig. 4. The results indicate that the corrosion current of the Ni–Mo–P deposit prepared in the electrolyte containing $4.13 \times 10^{-2}$ M sodium molybdate is the lowest and the corrosion resistance of this deposit is the best among these Ni–Mo–P coatings. In the case of adding $2.07 \times 10^{-2}$ M $Na_2MoO_4$ to the depositing solution (the lowest concentration of $MoO_4^{2-}$), the reduction rate of Ni and the deposition rate of Ni–Mo–P alloys are very fast. The Ni–Mo–P coating produced under such condition would possess coarse granules, a rough surface, large amount of defects, and inferior corrosion resistance. When the concentration of $Na_2MoO_4$ was increased to $4.13 \times 10^{-2}$ M in the depositing solution, the deposition rate of the Ni–Mo–P alloy reduced sharply.

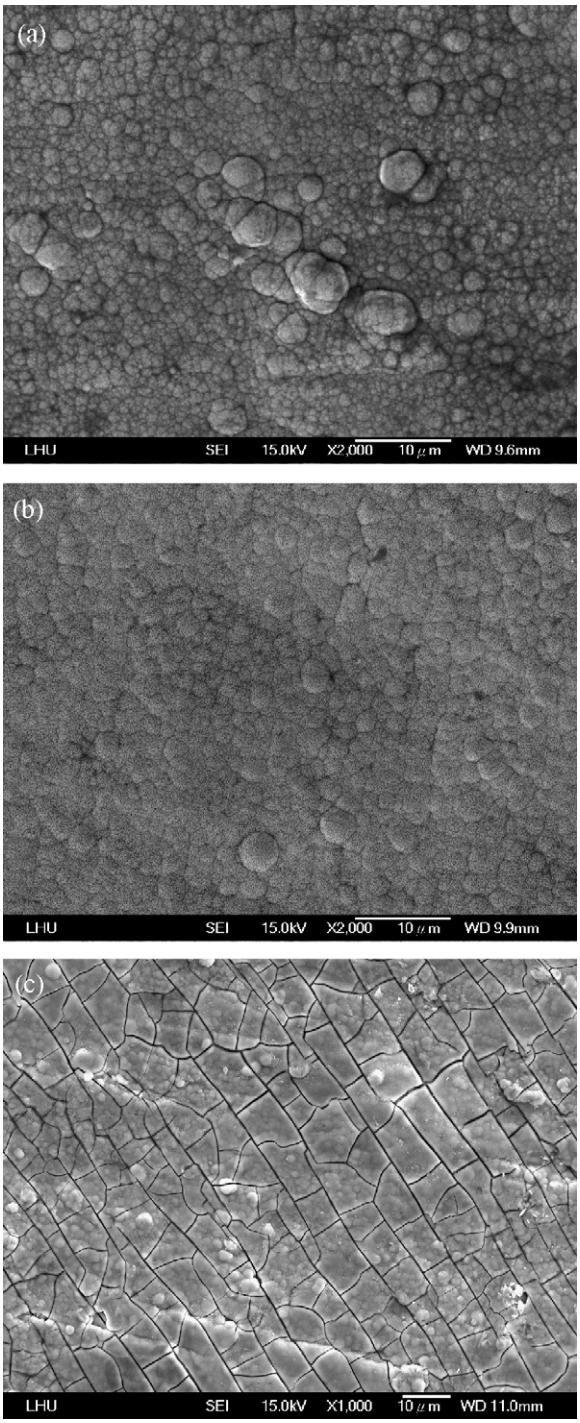


**Fig. 2.** The SEM topographies of the Ni–Mo–P alloys deposited in basic electrolytes (pH 9) with (a) $2.07 \times 10^{-2}$ M, (b) $4.13 \times 10^{-2}$ M, and (c) $6.20 \times 10^{-2}$ M $Na_2MoO_4$ at 70 °C.

Then, the deposit showed fine and dense granules, a smooth surface, and superior corrosion resistance. However, as the concentration of $Na_2MoO_4$ increased to $6.20 \times 10^{-2}$ M, the surface exhibits rough morphologies with many cracks. These cracks are induced by the release of the internal stress existing in the Ni–Mo–P alloy, because the coating contains excessive Mo. The corrosion media would attack the substrate through cracks of the Ni–Mo–P deposit. Therefore, the corrosion resistance of the Ni–Mo–P prepared in such condition is the worst among the three.

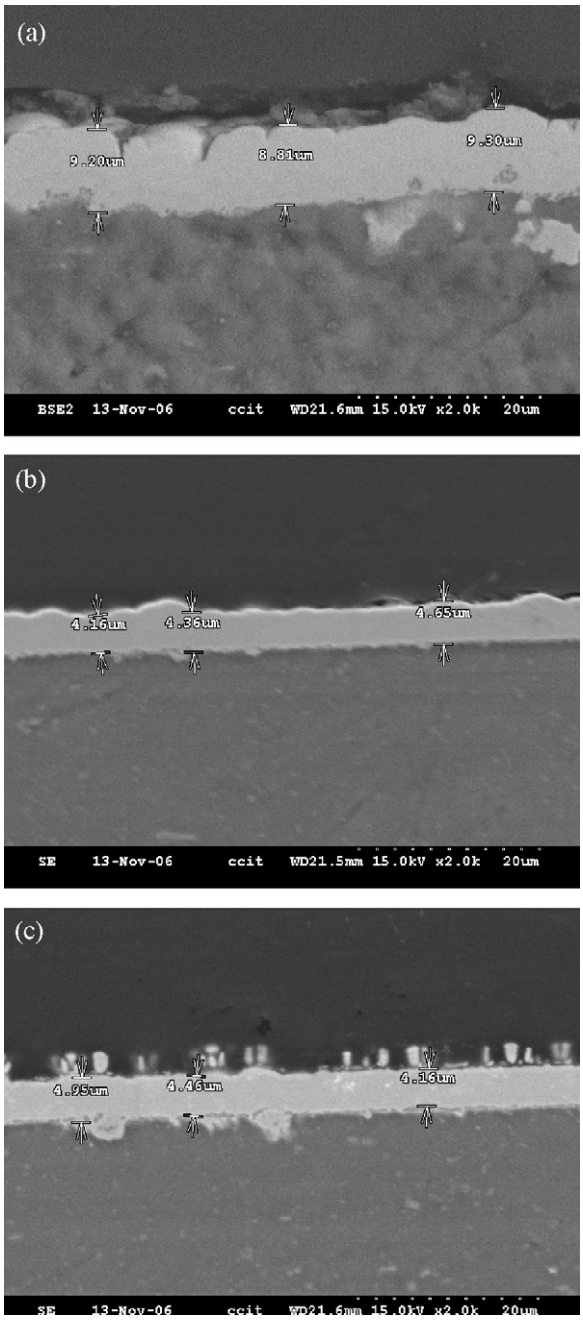


**Fig. 3.** Cross-sectional SEM images of the Ni–Mo–P alloys deposited in basic electrolytes (pH 9) with (a) $2.07 \times 10^{-2}$ M, (b) $4.13 \times 10^{-2}$ M, and (c) $6.20 \times 10^{-2}$ M $Na_2MoO_4$ at 70 °C.

### 3.2. Ni–Mo–P deposits prepared in different pH values

Fig. 5(a)–(c) shows the SEM topographies of the Ni–Mo–P deposits prepared in the solution containing $4.13 \times 10^{-2}$ M sodium molybdate at the pH values of 7, 8, and 9, respectively, for 1 h. The corresponding polarization curves of the Ni–Mo–P deposits tested in a 0.5 M $H_2SO_4$ solution are shown in Fig. 6(a)–(c). The surface morphologies of the Ni–Mo–P deposits reveal that the granule size increases with increasing pH values in the electroless bath. Moreover, the polarization measurement indicates that the corrosion resistance of Ni–Mo–P alloys declines with increasing pH values in the depositing solution. The reason for these phenomena is the difference in driving force of metal reduction or deposition in the solutions with various pH values.

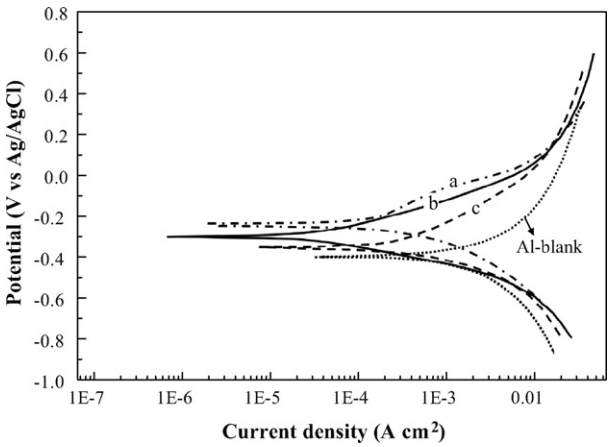


**Fig. 4.** The polarization curves of Ni–Mo–P deposits produced in electrolytes with (a) $2.07 \times 10^{-2}$ M, (b) $4.13 \times 10^{-2}$ M, and (c) $6.20 \times 10^{-2}$ M $Na_2MoO_4$.

The reduction possibility of Ni, Mo, and P depends strongly on the pH value in the solution. Higher concentration of hydroxide ions ($OH^-$) in the alkaline electrolytes will be beneficial for the oxidation of $HPO_2^-$ and the reduction of metal ions. On the contrary, lower concentration of $OH^-$ will be advantageous to the reaction of P reduction. In other words, the basic solution condition is helpful to the reaction of Ni and Mo reduction, and unfavorable to the precipitation of P [18,19]. Table 2 shows the composition percentage (wt.%) of Ni, Mo, and P detected by ICP-AES for the Ni–Mo–P deposits produced at the pH values of 7, 8, and 9. It can be confirmed that the contents of Ni and Mo in the Ni–Mo–P alloys would increase with increasing pH value of the electroless bath. However, a higher content of P in the ternary alloy would help to form an amorphous structure and thereby enhance its corrosion resistance [22,23]. If the content of phosphorus is low in the Ni–Mo–P alloys, the structure of the coatings may not be amorphous but polycrystalline. Moreover, the higher pH values, the faster growth rate of deposits, and hence the coarser granules. Therefore, the granules would be loosely packed with a lot of depositing defects, and the coating become more vulnerable to the attack by sulfuric acid solution. Accordingly, the corrosion resistance of the Ni–Mo–P prepared in higher pH bath is worse.

The polarization of the uncoated Al 5052 alloy tested in a 0.5 M $H_2SO_4$ solution is also shown in Figs. 4 and 6. The corrosion current is around $2.363 \times 10^{-4}$ A cm$^{-2}$, nearly in agreement with the testing result of a previous study [24]. Obviously the corrosion resistance of Al alloy is inferior, and Ni–Mo–P deposits can promote its corrosion resistance by at least 1–2 orders of magnitude.

### 3.3. Characteristics and the thermal stability of deposits

The estimated corrosion rates, tested in a 0.5 M $H_2SO_4$ solution, and the electrical resistivity, examined by a four-point probe sys-

**Table 2**
The composition percentage (wt.%) of Ni, Mo, and P in the Ni–Mo–P deposits produced at various pH values

| Conditions | Elements | | |
|---|---|---|---|
| | Ni | P | Mo |
| pH 7 | 90.1 | 6.8 | 3.1 |
| pH 8 | 90.6 | 5.3 | 4.1 |
| pH 9 | 89.8 | 3.9 | 6.3 |

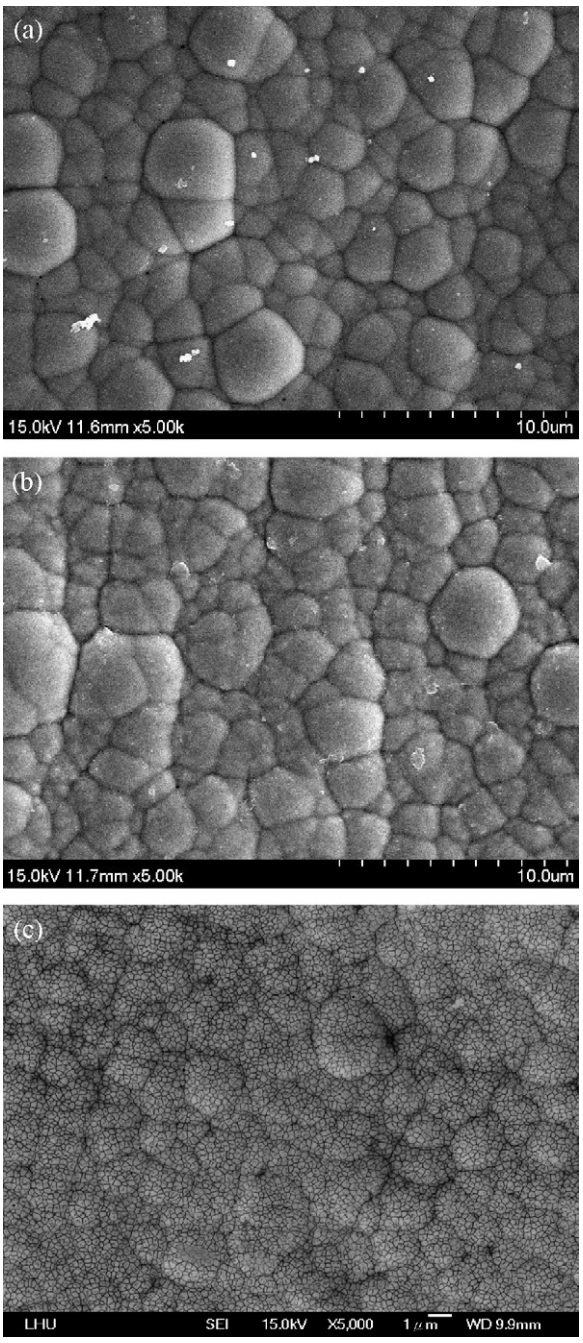


**Fig. 5.** The SEM topographies of the Ni–Mo–P deposits prepared in the solution containing $4.13 \times 10^{-2}$ M sodium molybdate at the pH values of (a) 7, (b) 8, and (c) 9.

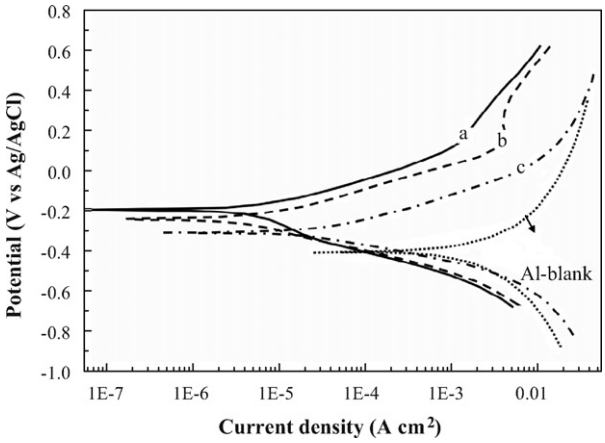


**Fig. 6.** The polarization curves of the Ni–Mo–P deposits prepared in the solution containing $4.13 \times 10^{-2}$ M sodium molybdate at the pH values of (a) 7, (b) 8, and (c) 9.

tem, of Ni–P or Ni–Mo–P alloys prepared in various conditions are listed in Table 3. It reveals that the Ni–Mo–P deposit, produced in the electrolyte (at pH 7) containing $4.13 \times 10^{-2}$ M sodium molybdate, possesses the most excellent corrosion resistance among all Ni–Mo–P alloys. The corrosion current and electrical conductivity of the U.S. Department of Energy (DOE) requirements for bipolar plates of PEMFC are 16 μA cm$^{-2}$ and 100 S cm$^{-2}$ at present, respectively. The suitable interfacial contact resistance (ICR), between bipolar plates (BPP) and gas diffusion layer (GDL), is 20 mΩ cm$^2$, when the testing loads at 140 N cm$^{-2}$. Evidently, the corrosion current and the electrical resistivity of the Ni–Mo–P alloy prepared under the optimum condition are comparable to those of the Ni–P deposit, and the electrical conductivity of all deposits produced in this experiment is superior to the DOE's target. Moreover, the addition of Mo in Ni–P alloys would significantly improve their thermal stability based on the results of the annealing experiment. Thermal stability is one of the important requirements on bipolar plates to extend the lifetime of fuel cells. To compare the thermal stability of the deposits, the Ni–P and the Ni–Mo–P prepared under the optimum condition were annealed at 400 °C, which is a more severe condition than the real case, for 1 h. The operating temperature is about 100 °C in the PEM fuel cell systems.

X-ray diffraction and hardness measurements were performed on the as-deposited or annealed Ni–P and Ni–Mo–P to examine the thermal stability of these deposits. Fig. 7 shows the XRD results of the Ni–P and Ni–Mo–P deposits. The diffraction pattern of the as-deposited Ni–P alloy, as seen in Fig. 7(a), shows an extremely broadened base with some identifiable peaks. It reveals that the as-deposited Ni–P alloy has a mixed structure composed of an amorphous matrix and some crystalline particles distributed in the matrix. However, the XRD result of the annealed Ni–P alloy, also shown in Fig. 7(a), demonstrates that the deposit obviously has become crystalline with Ni, $Ni_3P$, and $Ni_5P_2$ phases. The changes in

**Table 3**
The estimated corrosion rates and electrical resistance of Ni–P and Ni–Mo–P deposits prepared in various conditions

| Deposits | Conditions | | Properties | |
|---|---|---|---|---|
| | Concentrations of $Na_2MoO_4{\bullet}H_2O$ ($\times 10^{-2}$ M) | pH values | Corrosion rate (mm year$^{-1}$) | Resistivity (μ Ω cm) |
| Ni–P | – | 5 | 0.034 | 30.5 |
| Ni–Mo–P | 2.07 | 9 | 1.086 | 33.5 |
| | 4.13 | 9 | 0.923 | 23.1 |
| | 6.20 | 9 | 1.841 | 43.5 |
| | 4.13 | 7 | 0.038 | 29.3 |
| | 4.13 | 8 | 0.074 | 26.9 |

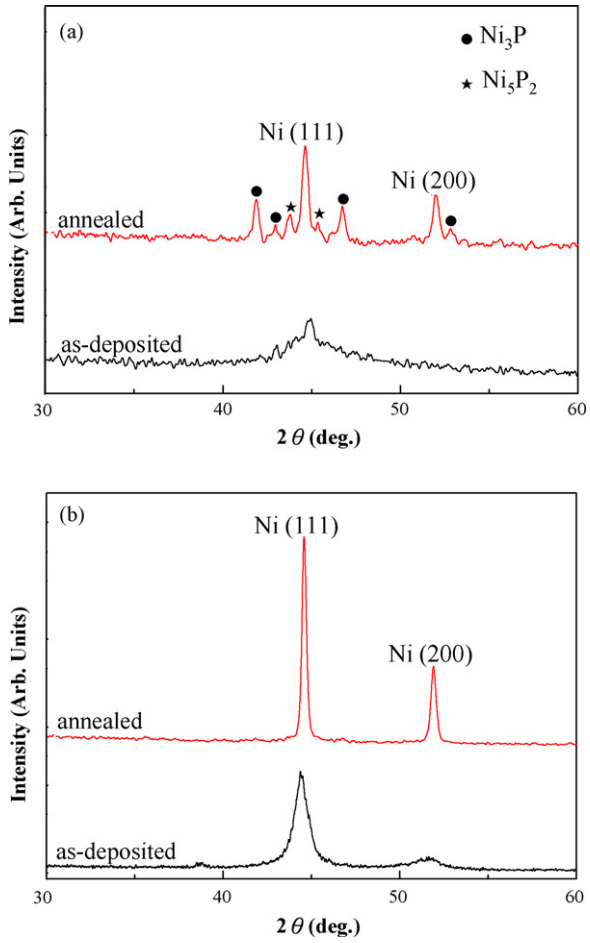


**Fig. 7.** XRD results of (a) the Ni–P and (b) the optimum Ni–Mo–P alloy in the as-deposited or the annealed states.

structures, constituents, and mechanical properties due to the heat treatment are evidently observed in the annealed Ni–P deposit. The measured hardness values of the as-plated and annealed Ni–P deposits are 542 HV and 919 HV, respectively. The great increase in hardness after annealing results from the formation of intermetallic precipitates, such as $Ni_3P$ and $Ni_5P_2$ phases, in the deposit. The intermetallic compounds with ordered structures cause the effect of precipitation hardening. However, the brittleness of the Ni–P deposit would increase with the amounts of precipitates. The enormous changes in the coating structures and constituents may also vary the dimension of coatings and induce some extent of deformations, and even weaken the bonding between the deposit and the substrate. Moreover, the corrosion resistance of the annealed Ni–P deposit would be inferior to that of the as-deposited coating because of the increase in grain boundaries and defects between the deposit and the substrate after the phase transformation.

On the contrary, the XRD patterns of the optimum Ni–Mo–P coatings in the as-deposited and the annealed states, shown in Fig. 7(b), both exhibit a crystallized structure with Ni(1 1 1) and Ni(2 0 0) diffraction peaks. The diffraction peaks of the as-deposited Ni–Mo–P are wider than those of the annealed one. Additionally, the measured hardness values for the as-deposited and annealed coatings are 446 HV and 433 HV, respectively, indicating that the hardness decreases slightly after annealing. These phenomena indicate that there are many as-deposited stresses or defects in the Ni–Mo–P alloy. Heat treatment helps to release the stress and reduce the defects. Therefore, the diffraction peaks become sharper, and the hardness becomes lower after annealing. Nevertheless, the constituent phases and the crystalline structure of the Ni–Mo–P alloys do not show apparent changes after annealing. It reveals that the Ni–Mo–P deposit produced in the optimum solution condition possesses good thermal stability because of the very low mobility of Mo, which restrains the phase or constituent transformation.

The excellent thermal stability of the Ni–Mo–P alloy can be further confirmed with the corrosion tests. The polarization curves, measured in a 0.5 M $H_2SO_4$ environment, of the deposits in the as-plated or the annealed states are shown in Fig. 8. The corrosion currents (Icor.) of the as-deposited and the annealed Ni–P deposit are $3.00 \times 10^{-6}$ A cm$^{-2}$ and $1.52 \times 10^{-5}$ A cm$^{-2}$, respectively. The corrosion current of the Ni–P coating is substantially higher after annealing. The poor corrosion resistance of the annealed Ni–P deposits is induced by the precipitation of intermetallics and the increase of grain boundaries. On the other hand, the acceleration of corrosion rate in the optimum Ni–Mo–P deposit is hardly noticeable after the annealing treatment: the corrosion currents before and after annealing are $3.38 \times 10^{-6}$ A cm$^{-2}$ and $6.04 \times 10^{-6}$ A cm$^{-2}$, respectively. Based on these results, obviously Ni–Mo–P coatings will offer better corrosion resistance than Ni–P when the bipolar plates are heated during the fuel cell operation.

### 3.4. Corrosion behaviors of deposits in different environments and long-term corrosion resistance

PEMFCs rely on the transport of $H^+$ ions to carry on the oxidation–reduction reaction of the fuel cell. The electrolyte in a PEMFC system is a solid acid membrane saturated with water, and

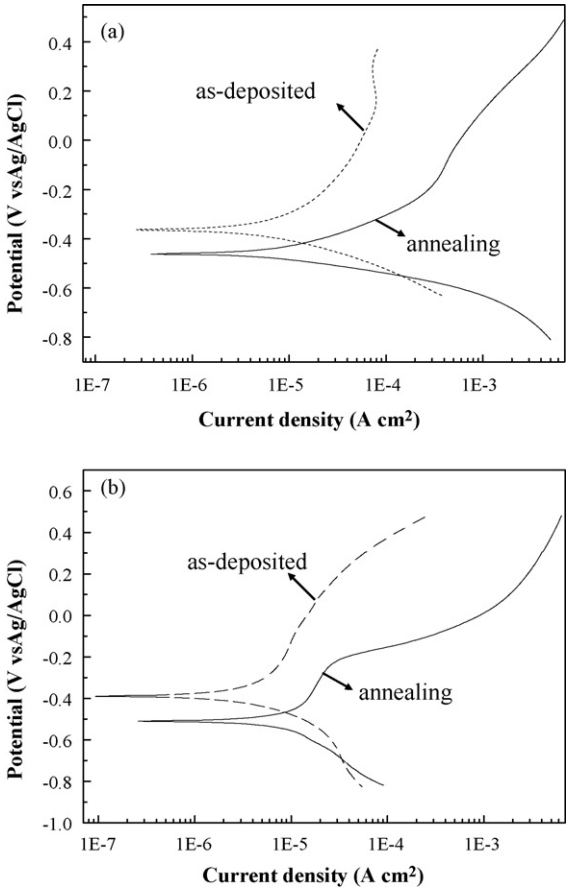


**Fig. 8.** The polarization curves of (a) the Ni–P and (b) the optimum Ni–Mo–P deposit in the as-deposited or the annealed states tested in 0.5 M $H_2SO_4$ solution.

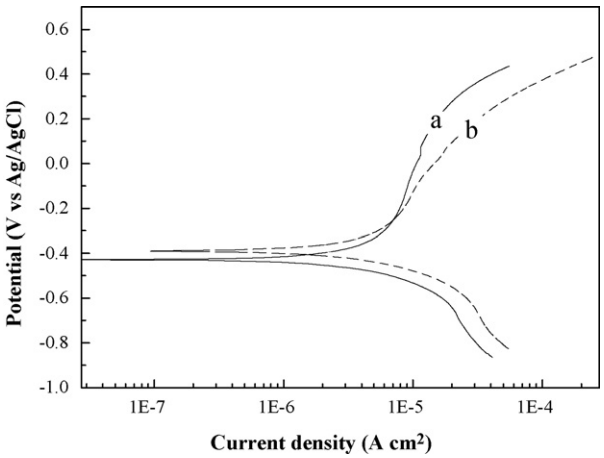


**Fig. 9.** The polarization curves of (a) the Ni–P and (b) the optimum Ni–Mo–P deposit tested in a 3.5% saltwater solution.

the solutions in the cell are composed mainly of $H_2SO_4$ aqueous solution mixed with some $F^-$ and other ions. The bipolar plates, therefore, would be attacked by different corrosion media and have to possess excellent corrosion resistance in various environments to keep the performance of fuel cells. For this reason, the aqueous solutions of (1) 3.5% saltwater, (2) 0.5 M $H_2SO_4$, or (3) 0.5 M $H_2SO_4$ + 10 ppm HF are used as corrosion electrolytes to evaluate the corrosion resistance of the Ni–P and the optimum Ni–Mo–P coatings in attacking environments.

Fig. 9 shows the polarization curves of the Ni–P and the optimum Ni–Mo–P deposits tested in a 3.5% saltwater solution. The corrosion currents of the two deposits are $1.30 \times 10^{-6}$ A cm$^{-2}$ and $1.75 \times 10^{-6}$ A cm$^{-2}$, respectively. It indicates that both the Ni–P and the Ni–Mo–P deposits are difficult to dissolve and have outstanding corrosion resistance in neutral electrolytes. The corrosion currents of the as-deposited Ni–P and optimum Ni–Mo–P deposits tested in a 0.5 M $H_2SO_4$ are $3.00 \times 10^{-6}$ A cm$^{-2}$ and $3.38 \times 10^{-6}$ A cm$^{-2}$, respectively. The testing results are shown in Fig. 8(a) and (b). The corrosion current of the deposits tested in a 0.5 M $H_2SO_4$ is higher than those in a 3.5% saltwater solution, indicating that the corrosion resistances of the Ni–P and Ni–Mo–P alloys are slightly worse in acidic electrolytes. The polarization curves of the Ni–P and the Ni–Mo–P deposits examined in a 0.5 M $H_2SO_4$ + 10 ppm HF solution are shown in Fig. 10. The corrosion currents of the Ni–P and the Ni–Mo–P deposits in such a mixed acid are $5.03 \times 10^{-6}$ A cm$^{-2}$ and $4.78 \times 10^{-6}$ A cm$^{-2}$, respectively. The corrosion attack of a mixed acid solution on the alloys is more severe than that of a single acid environment. The corrosion resistances of the Ni–P and the Ni–Mo–P deposits in a mixed acid solution of 0.5 M $H_2SO_4$ + 10 ppm HF are worse than those in a 0.5 M $H_2SO_4$ environment. Furthermore, the corrosion resistance of the Ni–Mo–P deposits in such a mixed acid solution is better than that of the Ni–P deposits. Therefore, Ni–Mo–P alloys are more suitable as bipolar plates in PEM fuel cells than Ni–P.

Additionally, most of metal bipolar plates exhibit an insufficiency of long-term corrosion resistance, and the metal ions dissolving in the electrolyte would poison the polymer membrane. The coatings of bipolar plates, therefore, have to possess superior and enduring corrosion resistance in attacking environments to increase the performance and service life of fuel cells. Hence, the Ni–P and the Ni–Mo–P deposits were immersed in a 0.5 M $H_2SO_4$ solution for 20 h or 40 h and then polarized in the same electrolyte, as shown in Fig. 11. The corrosion currents of the Ni–P and the optimum Ni–Mo–P deposits immersed in a 0.5 M $H_2SO_4$ solution for 20 h are $5.26 \times 10^{-5}$ A cm$^{-2}$ and $1.51 \times 10^{-5}$ A cm$^{-2}$, respectively. The corresponding corrosion currents for 40-h immersion are $8.25 \times 10^{-4}$ A cm$^{-2}$ and $3.225 \times 10^{-5}$ A cm$^{-2}$, respectively.

The results indicate that their corrosion resistance both degrades after soaking in a 0.5 M $H_2SO_4$ solution for a long time, but the Ni–Mo–P deposit outperforms the Ni–P coating. It has been pointed out that the long-term corrosion resistance of Ni–Mo–P alloys can be remarkably improved by forming dense Mo oxide

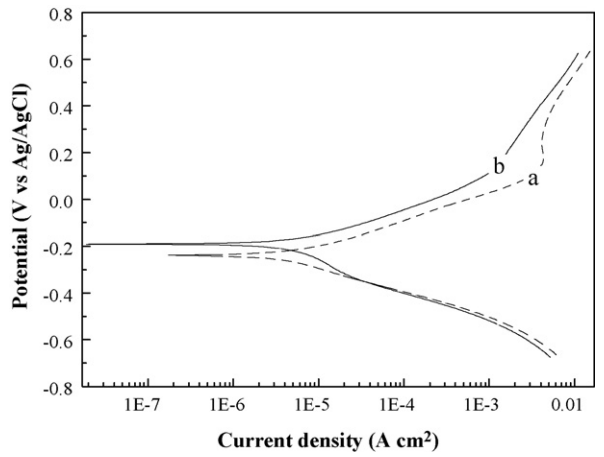


**Fig. 10.** The polarization curves of (a) the Ni–P and (b) the Ni–Mo–P deposits tested in a 0.5 M $H_2SO_4$ + 10 ppm HF solution.

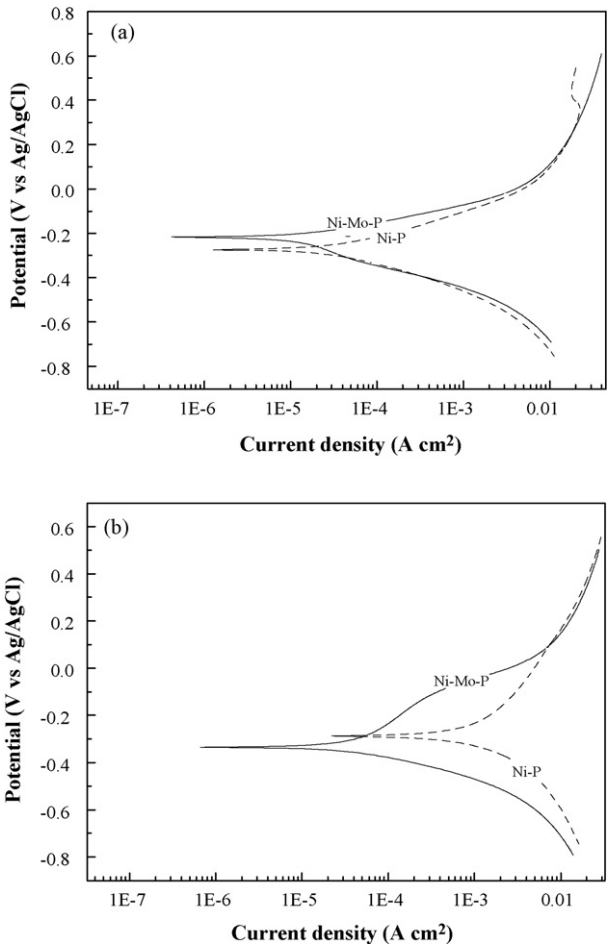


**Fig. 11.** The polarization curves of the Ni–P and the Ni–Mo–P deposits after immersing in a 0.5 M $H_2SO_4$ for (a) 20 h and (b) 40 h.

films on the deposit [23,25]. Moreover, the passive Mo element would accumulate on the grain boundaries of the Ni–Mo–P coating and result in a stuffing effect [18,26], which prevents the corrosion media and the metal ions from diffusing via grain boundaries. Therefore, the Ni–Mo–P deposit has better long-term corrosion resistance in a 0.5 M $H_2SO_4$ environment.

In summary, the experimental results show that the optimum Ni–Mo–P coatings can improve the conductivity and the chemical characteristics of Al-alloys to surpass the requirements for metal bipolar plates. Therefore, Ni–Mo–P deposits have a potential to be used as the coating material for bipolar plates in PEM fuel cells. However, the improvement in the chemical properties of the deposits by adding Mo is not very apparent. The reason is that the contents of both Mo and P in these Ni–Mo–P alloys are too low to noticeably enhance the corrosion resistance of the deposits. It is very difficult to produce a Ni–Mo–P deposit with high contents of both Mo and P using the traditional electroless plating method. Fortunately, a novel technology named non-isothermal deposition (NITD) system has been used to produce Ni–Mo–P deposits concomitantly with high contents of Mo and P in our previous work [27]. The NITD technique will be employed to prepare Ni–Mo–P coating for Al-alloy bipolar plates in our future work, and hopefully the performance will be further enhanced.

## 4. Conclusions

The deposit produced in the electrolyte with $4.13 \times 10^{-2}$ M $Na_2MoO_4$ at the pH value of 7.0 showed the finest and densest surface conditions among the Ni–Mo–P alloys prepared in various concentrations of $Na_2MoO_4$. The thickness, the granule size, and the surface roughness of Ni–Mo–P coatings prepared in the electroless bath decrease with increasing concentration of $Na_2MoO_4$. The ranking of the concentration of $Na_2MoO_4$, according to the corrosion resistance and conductivity in the Ni–Mo–P alloys, from best to worst, is as follows: $4.13 \times 10^{-2}$ M, $2.07 \times 10^{-2}$ M, and $6.20 \times 10^{-2}$ M.

The higher the pH values, the larger the driving force for Ni reduction. Therefore, the granule size and the depositing defects of the Ni–Mo–P alloys would increase with the pH values in a basic depositing system. When testing in a dilute sulfuric acid solution, the corrosion resistance of the Ni–Mo–P prepared in solutions with higher pH values is worse than those formed at lower pH values.

Based on the experimental results, a high-quality Ni–Mo–P coating for Al-alloy bipolar plates can be produced by regulating the pH value and the concentration of $Na_2MoO_4$ in the depositing solution. The optimum controlling conditions of electroless bath to fabricate Ni–Mo–P deposits are $4.13 \times 10^{-2}$ M $Na_2MoO_4$ at the pH values of 7.0 and the temperature of 70 °C for the best performances in the thermal stability and the corrosion resistance. Compared to Ni–P, the optimum Ni–Mo–P alloy shows a better thermal stability. In addition, the corrosion resistance of the optimum Ni–Mo–P alloy is better than that of the Ni–P coatings, when the two deposits are tested in a mixed acid solution of 0.5 M $H_2SO_4$ + 10 ppm HF or after soaking in a dilute $H_2SO_4$ solution for a long time. Therefore, Ni–Mo–P alloys are more suitable to be used as the coating material for bipolar plates in fuel cells than Ni–P deposits.

## References

[1] B.C.H. Steele, A. Heinzel, Nature 414 (2001) 345–352.
[2] R.L. Borup, N.E. Vanderborgh, Mater. Res. Soc. Symp. Proc. 393 (1995) 151–155.
[3] A. Hermann, T. Chaudhuri, P. Spagnol, Int. J. Hydrogen Energy 30 (2005) 1297–1302.
[4] M.H. Oh, Y.S. Yoon, S.G. Park, Electrochim. Acta 50 (2004) 777–780.
[5] H. Tawfika, Y. Hung, D. Mahajan, J. Power Sources 163 (2007) 755–767.
[6] H. Tsuchiya, O. Kobayashi, Int. J. Hydrogen Energy 29 (2004) 985–990.
[7] D.R. Hodgson, B. May, P.L. Adcock, D.P. Davies, J. Power Sources 96 (2001) 233–235.
[8] D.P. Davis, P.L. Adcock, M. Turpin, S.J. Rowen, J. Power Sources 86 (2000) 237–242.
[9] J. Wind, R. Späh, W. Kaiser, G. Böhm, J. Power Sources 105 (2002) 256–260.
[10] J. Jayaraj, Y.C. Kim, K.B. Kim, H.K. Seok, E. Fleury, Sci. Technol. Adv. Mater. 6 (2005) 282–289.
[11] S.J. Lee, C.H. Huang, Y.P. Chen, Y.M. Chen, J. Fuel Cell Sci. Technol. 2 (2005) 208–212.
[12] H. Wang, J.A. Turner, J. Power Sources 128 (2004) 193–200.
[13] E. Fleury, J. Jayaraj, Y.C. Kim, H.K. Seok, K.Y. Kim, K.B. Kim, J. Power Sources 159 (2006) 34–37.
[14] J.W. Schultze, A. Bressel, Electrochem. Acta 47 (2001) 3–21.
[15] T. Homma, I. Komatsu, A. Ttamaki, H. Nakai, T. Osaka, Electrochem. Acta 47 (2001) 47–53.
[16] S. Furukawa, M. Mehregany, Sens. Actuators A 56 (1996) 261–266.
[17] N. Takano, N. Hosoda, T. Yamada, T. Osaka, J. Electrochem. Soc. 146 (1999) 1407–1411.
[18] Y. Wu, C.C. Wan, Y.Y. Wang, J. Electron. Mater. 34 (2005) 541–550.
[19] G. Lu, G. Zangari, J. Electrochem. Soc. 150 (2003) C777–C786.
[20] Y. Wang, D.O. Northwood, J. Power Sources 165 (2007) 293–298.
[21] Y. Fu, M. Hou, G. Lin, J. Hou, Z. Shao, B. Yi, J. Power Sources 176 (2008) 282–286.
[22] A. Kohn, M. Eizenberg, Y. Shacham-Diamand, J. Appl. Phys. 94 (2003) 3810–3822.
[23] Y. Gao, Z.J. Zheng, M. Zhu, C.P. Luo, Mater. Sci. Eng. A 381 (2004) 98–103.
[24] S.J. Lee, C.H. Huang, Y.P. Chen, J. Mater. Process. Technol. 140 (2003) 688–693.
[25] H. Lou, S. Zhu, F. Wang, Oxid. Met. 43 (1995) 317–328.
[26] M.A. Nicolet, Thin Solid Films 52 (1978) 415–443.
[27] Y.H. Chou, Y. Sung, K.L. Ou, Y.M. Liu, M.D. Ger, Electrochem. Solid-State Lett. 11 (2008) D30–D33.